ELSEVIER

Biochimica et Biophysica Acta 1279 (1996) 25–34

BBA Biochimica et Biophysica Acta

Triggerable plasmalogen liposomes: improvement of system efficiency

David H. Thompson *, Oleg V. Gerasimov [1], Jefferey J. Wheeler [2], Yuanjin Rui, Valerie C. Anderson [3]

Department of Chemistry Purdue University, West Lafayette, IN 47907-1393, USA

Received 27 December 1994; revised 26 June 1995; accepted 15 August 1995

Abstract

A photoactivated liposome release system that is generally applicable for triggered release of encapsulated hydrophilic materials is described. This approach to phototriggered release, derived from the known effects of plasmalogen photooxidation on membrane permeability in whole cells and model membrane systems, relies on producing a lamellar phase change or increase in permeability upon cleaving its constitutive lipids to single-chain surfactants using 630–820 nm light to sensitize the photooxidation of the plasmalogen vinyl ether linkage. Semi-synthetic plasmenylcholine liposomes containing encapsulated calcein and a membrane-bound sensitizer, such as zinc phthalocyanine, tin octabutoxyphthalocyanine, or bacteriochlorophyll *a*, were prepared by extrusion. Irradiation of air-saturated liposome solutions enhanced membrane permeability toward calcein and Mn^{2+}, and promoted membrane fusion processes compared to non-irradiated or anaerobic controls. Bacteriochlorophyll *a* sensitization produced the fastest observed photoinitiated release rate from these liposomes (100% calcein release in less than 20 min; 800 nm irradiation at 300 mW); the observed release rate was two orders of magnitude slower for egg lecithin liposomes prepared and irradiated under identical experimental conditions. Liposome aggregation, interlipidic particle formation, and membrane fusion between adjoining liposomes was observed by ^{31}P-NMR, freeze-fracture/freeze-etch TEM, and cryo-TEM as a function of irradiation time. The use of near-infrared sensitizers and the capacity of photolyzed plasmenylcholine liposomes to undergo membrane fusion processes make photodynamic therapy with these liposome-borne sensitizers an attractive adjunct to biochemical targeting methods.

Keywords: Controlled release; Drug delivery; Electron microscopy; Interlipidic particle; Light-triggerable liposome; Liposome; Photodynamic therapy; Photooxidation; Plasmalogen

1. Introduction

Despite many years of investigation, selective targeting and membrane translocation of drugs to specific cell targets in the body remains one of the most difficult problems in pharmaceutics. Immunoconjugation and hydrophobization have been widely pursued means of addressing these problems; however, both of these tactics can lead to decreased efficacy of the drug. Liposomes have undergone intensive development as drug delivery vehicles due to their ability to efficiently encapsulate antitumor agents in high concentrations [1], circulate in the blood for periods of 24 h or more [2–5], and deposit at target tissue sites by a variety of biochemical [6,7] and physical [8,9] targeting mechanisms. Unfortunately, the scope of liposome targeting is presently limited by the tight endothelial lining and basement membrane of healthy vasculature which presents a mechanical barrier to systemically circulating particles. As a result, multilamellar and large unilamellar liposomes tend to localize in the reticuloendothelial system and, eventually, in the liver, spleen, and bone marrow. Much of the recent work, therefore, has focused on increasing circulation times without inhibiting the reticuloendothelial system (by modification of liposome parameters such as particle size, lipid composition/surface charge, and

Abbreviations: BChla, bacteriochlorophyll *a*; lysolipid, 2-palmitoyl-*sn*-glycero-3-phosphocholine; PlsPamCho, 1-alk-1′-enyl-2-palmitoyl-*sn*-glycero-3-phosphocholine; $SnCl_2Pc(OBu)_8$, tin(IV) 1,4,8,11,15,18,22,25-octabutoxyphthalocyanine dichloride; TEM, transmission electron microscopy; TLC, thin-layer chromatography; ZnPc, zinc phthalocyanine.

* Corresponding author. Fax: +1 (317) 4962592; e-mail: davethom@chem.purdue.edu.

[1] Visiting Scientist. Permanent address: Institute of Catalysis, Siberian Branch of the Russian Academy of Sciences, Pr. Ak. Lavrentieva 5, Novosibirsk 630090, Russia.

[2] Present address: INEX Pharmaceutical, 1779 West 75th Avenue, Vancouver, BC, V6P 6P2, Canada.

[3] Present address: Division of Neurosurgery, Oregon Health Sciences University, Portland, OR 97201, USA.

SSDI 0005-2736(95)00210-3

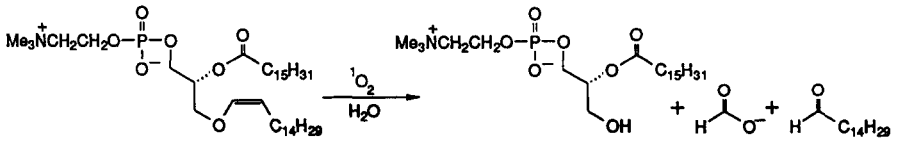

Fig. 1. Singlet oxygen-mediated photooxidation of plasmalogen vinyl ether linkage.

drug:lipid loading) and on improving targeting methods to sites with compromised vasculature. Recently reported formulations incorporating minor proportions of gangliosides or polyethylene glycol-derivatized lipids (sterically stabilized or Stealth® liposomes) have obviated many of these problems [10–13]. These efforts have lead to an increased uptake of doxorubicin loaded liposomes at tumor sites [9] and tumor regression in a mouse model [14]. Triggering mechanisms are now needed to increase the otherwise slow passive release from these particles to improve their pharmacokinetics.

A wide variety of liposomal release mechanisms activated by light, heat, low pH, or enzymatic activity have been reported; these approaches have been extensively reviewed [15–18]. One of these methods, doxorubicin delivery from temperature-sensitive liposomes near implanted murine tumors, has lead to inhibition of tumor growth upon microwave-activation of the drug loaded liposomes at the tumor site [19,20]. Photoactivated liposome release, however, is the most flexible of the existing triggering methods since (i) a wide variety of tissues can be irradiated endoscopically, especially using near-infrared wavelengths [21,22], (ii) light intensity and modulation are externally controllable variables that can be manipulated as required for optimal drug delivery [23–25], and (iii) the applied excitation energy can be effectively confined at the target site [18]. Although photochemical activation of light-sensitive liposomes can, in principle, trigger contents release with a relatively high degree of temporal- and site-specificity under appropriate conditions, constraints such as plasma stability, near-infrared sensitivity, and biocompatibility have limited the development of a practical light-sensitive liposome formulation.

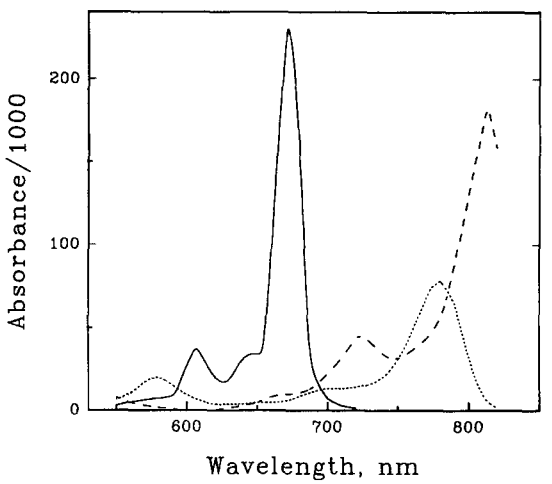

Fig. 2. Molar absorbance of sensitizers used in the irradiation experiments. Solid line: ZnPc in benzene; dashed line: $SnCl_2Pc(OBu)_8$ in $CHCl_3$; dotted line: BChla in $CHCl_3$.

We recently reported a strategy for photoactivated liposomal contents release that appears broadly applicable to the challenge of site- and/or time-specific drug delivery [26,27]. This approach, derived from the known effects of plasmalogen photooxidation on membrane permeability in whole cells [28,29] and model membrane systems [30] relies on producing a change in membrane phase or permeability upon cleavage of plasmenylcholine to single chain surfactants via sensitized photooxidation of the plasmalogen vinyl ether linkage (Fig. 1).

This report presents release kinetics for phototriggered plasmenylcholine liposomes using three different sensitizers absorbing between 630 and 820 nm (Fig. 2). We have chosen this wavelength regime for sensitization of the liposome photochemistry since (i) penetration depths of this wavelength are ≥ 0.8 cm in many tissues [23–25], (ii) sensitizers absorbing in this wavelength region are commercially available, (iii) high-power light sources emitting in this wavelength range (e.g. Al/Ga/As laser diodes) are available at relatively low cost, and (iv) by hybridizing liposomal and photodynamic therapy technologies, it should be possible to exert a synergistic lethal effect by carrying encapsulated antitumor agents and membrane-bound photodynamic sensitizers to the target tissue for site-selective deposition and light-activated release. Morphological changes in the liposome dispersions during the course of photolysis have also been characterized by electron microscopy and ^{31}P-NMR. A conceptual model for photoinduced liposome leakage and fusion based on our observations is also proposed.

2. Materials and methods

2.1. Reagents

Semi-synthetic plasmenylcholine (PlsPamCho) used in this study was prepared from bovine heart choline glycerophospholipids (bovine heart L-α-phosphatidylcholine; Avanti Polar Lipids) as previously described [26]. Tin(IV) 1,4,8,11,15,18,22,25-octabutoxyphthalocyanine dichloride ($SnCl_2Pc(OBu)_8$) was prepared according to published methods [31]. Egg lecithin (egg L-α-phosphatidylcholine; Avanti Polar Lipids), bacteriochlorophyll *a* (BChla; Por-

phyrin Products and Sigma), zinc phthalocyanine (ZnPc; Aldrich), tris(hydroxymethyl)aminomethane (Tris, Aldrich), NaCl, and chromatographically-purified calcein (Molecular Probes) were used as received.

Solutions of BChla in chloroform (1 mg/5 ml) were freshly prepared. All manipulations with BChla solutions were carried out in a dimly lit room.

2.2. Liposome preparation

ZnPc/PlsPamCho liposomes were prepared as described previously [26]. BChla- and $SnCl_2Pc(OBu)_8$-containing liposomes were prepared by adding an aliquot of sensitizer stock solution to a known amount of PlsPamCho in a 10 mm test tube (typically 1 ml of sensitizer stock into 14 mg of PlsPamCho). The chloroform was evaporated under a N_2 flow and the traces of solvent removed under vacuum (0.1 torr) for 6 h. The lipid was hydrated in calcein solution (50 mM, pH 12.5) using 5 cycles of freezing (liquid nitrogen)-thawing-vortexing and then extruded 10 times at 45°C through two stacked Nuclepore filters (pore diameter either 0.08 μm or 0.1 μm as noted) using a Lipex Biomembranes Extruder to form large unilamellar liposomes [32]. The external liposomal solution was exchanged with 100 mM NaCl/20 mM Tris, pH 8.0, using a 1 × 40-cm Sephadex G-50-150 column. Dark leakage rates from the liposomes did not exceed 10%, and were typically much slower than the time scale of our experiments (i.e., ~ 6 h). Non-illuminated samples were stable in the dark for more than a week.

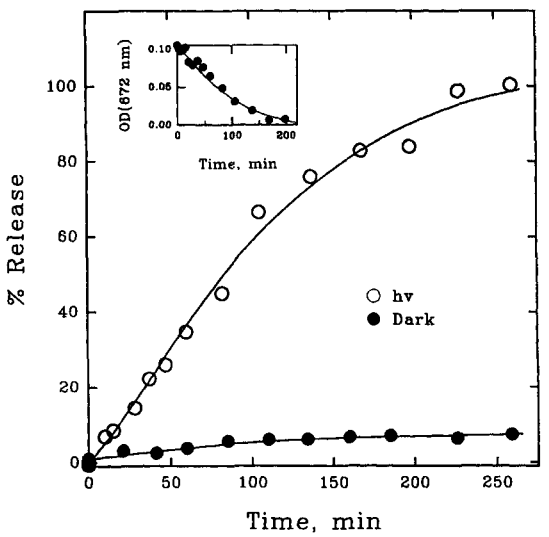

Fig. 3. ZnPc-sensitized release of calcein from PlsPamCho liposomes (8 μM ZnPc, 13.9 mM PlsPamCho in 100 mM NaCl/20 mM Tris) irradiated at 39°C ($\lambda > 640$ nm, incident light power 80 mW/cm^2, illuminated area = 2 cm^2). ○, light-induced release; ●, dark control. (Inset) ZnPc photobleaching rate monitored at 672 nm (12-fold dilution of liposome solution).

2.3. Liposome release assay

A 10-μl aliquot of the liposome solution was taken at various times, dissolved in 3 ml of 100 mM NaCl/20 mM Tris, and the calcein fluorescence intensity measured (λ_{ex} = 490 nm, λ_{em} = 518 nm) using a Perkin-Elmer MPF-66 Spectrofluorimeter. This procedure gave a linear relationship between the amount of calcein released and the observed fluorescence intensity over the concentration range employed. The extent of liposomal leakage was then compared with the 100% release value (determined by addition of Triton X-100 to the diluted liposome sample) and expressed as a percentage. Calcein fluorescence measurements for individual data points during the photolysis experiments varied by ±20%; batch-to-batch reproducibility was observed to be within these experimental limits.

2.4. Photolysis conditions

Samples to be illuminated were transferred to a 1-cm quartz cuvette and the contents continuously stirred in a thermostated cuvette holder; the cuvette was left unstoppered to allow for interfacial gas exchange at all times. The light from an Oriel 250 W quartz tungsten halogen lamp, filtered with a 10-cm water cell (IR filter) and a OG630 cutoff filter, was used for irradiation of ZnPc-containing liposomes. All other samples were illuminated using a SDL 820 diode laser (Spectra Diode Labs, San Jose, CA, $\lambda_{em} \approx 800$ nm) via optical fiber, the emitting end of which was mounted perpendicular to the cuvette window to produce an incident light spot of approx. 3-mm diameter. Incident light intensities were measured using a MAX5100 power meter (Molectron Detector, Portland, OR). All illuminations were performed at 38–39°C where phase transition effects on the leakage rate from PlsPamCho liposomes are negligible [33].

2.5. Analysis of photoproducts

Thin-layer chromatography (TLC) analysis of the photolysis products was carried out as described earlier [26].

2.6. Electron microscopy

2.6.1. Freeze-fracture electron microscopy

Freeze-fracture replicas were prepared as described by Hope et al. [34] using a Balzers BAF400 apparatus and imaged using a JEOL JEM-1200EX microscope. The samples were freeze-etched prior to carbon coating and platinum shadowing by exposing the sample for 2 min to high vacuum at −90°C immediately after fracturing.

2.6.2. Cryo-electron microscopy

A drop of lipid suspension was applied to bare 700 mesh gold EM grids (previously treated by 15 s glow-discharge) and the excess removed by blotting with filter

paper. The sample was then rapidly frozen in liquid propane cooled to −187°C [35] and transferred via a Reichart-Jung KF80 Universal Cryo-fixation system to a Gatan 126 cold stage cooled with liquid nitrogen; the vitreous sample was then visualized using a Zeiss EM 10C STEM operating at 60–80 kV.

2.7. NMR spectroscopy

Tris buffered solutions of lipid (30 mg/ml) were placed in 10 mm NMR tubes and 100 μl of D_2O added. ^{31}P-NMR spectra were acquired using a Bruker MSL 200P spectrometer; 6000 transients were collected using a 5-μs pulse (1 s

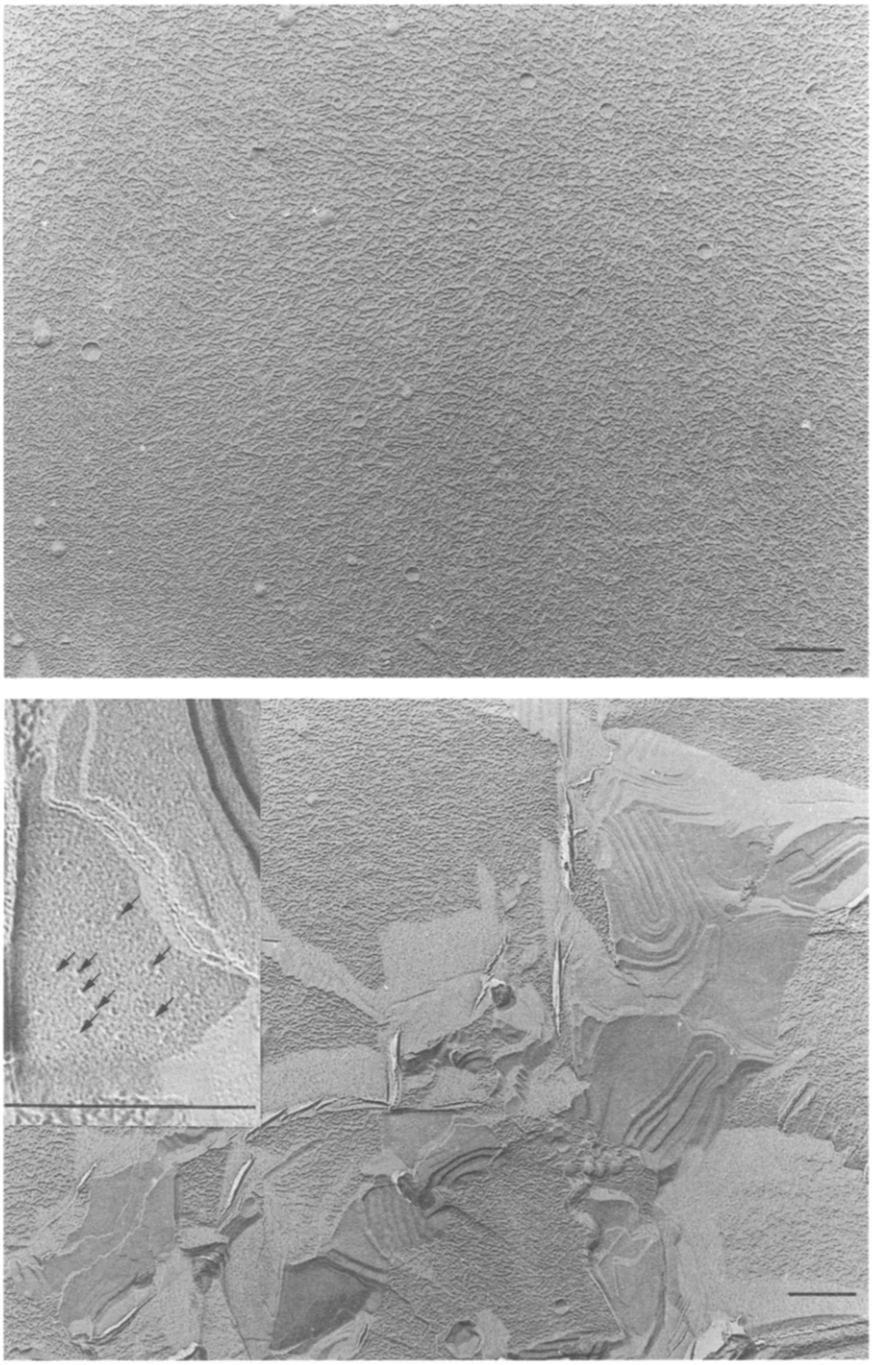

Fig. 4. Freeze-fracture/freeze-etch microscopy of extruded ZnPc/PlsPamCho (0.7 μM ZnP, 5 mM PlsPamCho in 100 mM NaCl/20 mM Tris) liposomes. (Top) Before irradiation; mean liposome diameter = 865 Å by quasielastic light scattering analysis. (Bottom) ZnPc/PlsPamCho liposomes 24 h after 90 min broadband illumination (see legend to Fig. 3). (Bottom, inset at top, left) Enlargement of the central portion of the micrograph (B). Arrows indicate interlipidic particles. Scale bars = 2000 Å.

delay) and processed using 10 Hz and 50 Hz linebroadening for the nonirradiated and irradiated samples, respectively. Manganese chloride (200 mM, pH 5.5) was added by microliter syringe to give a final concentration of 5 mM and vortexed prior to reacquisition of the spectrum. Particle size changes were verified by quasielastic light scattering using a Nicomp Model 270 instrument.

3. Results and discussion

3.1. Kinetics of calcein release from PlsPamCho liposomes

3.1.1. ZnPc sensitization

Photoinduced release of encapsulated calcein from ZnPc/PlsPamCho liposomes is shown in Fig. 3. Calcein release is accompanied by complete photobleaching of ZnPc within 150 min (Fig. 3, inset). Gross morphological transformation (Fig. 4) from small unilamellar liposomes to multilamellar sheets occurred as detected by freeze-fracture/freeze-etch TEM. This shape transformation presumably results from large scale liposome-liposome fusion events initiated during the course of photoexcitation and continuing throughout the 24 h dark incubation period preceding TEM analysis. The exposed lamellar surfaces reveal spherical defect structures with 50–120 Å diameters (Fig. 4, inset). We attribute these lamellar defects to interlipidic particles [36] that form as a consequence of plasmenylcholine degradation to single chain surfactants which stabilize hexagonal phase domains within the membrane [37].

3.1.2. $SnCl_2Pc(OBu)_8$ sensitization

The kinetics of calcein release for $SnCl_2Pc(OBu)_8$-containing liposomes are shown in Fig. 5. This sensitizer was chosen due to its favorable absorption cross section (Fig. 2) with Ga/Al/As laser sources. Aerobic irradiation of $SnCl_2Pc(OBu)_8$-containing liposomes at 800 nm resulted in 100% release of entrapped calcein over a 6 h period (and > 90% bleaching of the chromophore) compared with 10% release of calcein during the same time interval for non-irradiated PlsPamCho liposomes.

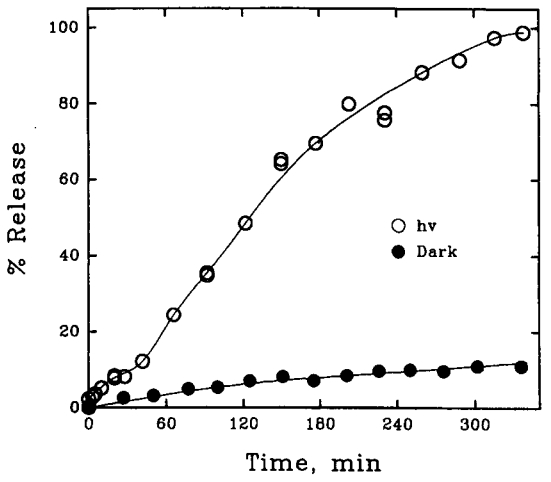

Fig. 5. $SnCl_2Pc(OBu)_8$-sensitized release of calcein from PlsPamCho liposomes (1 μM SnPc, 13.9 mM PlsPamCho in 100 mM NaCl/20 mM Tris) irradiated at 38°C (λ = 800 nm, incident light power 300 mW). ○, light-induced release; ●, dark control.

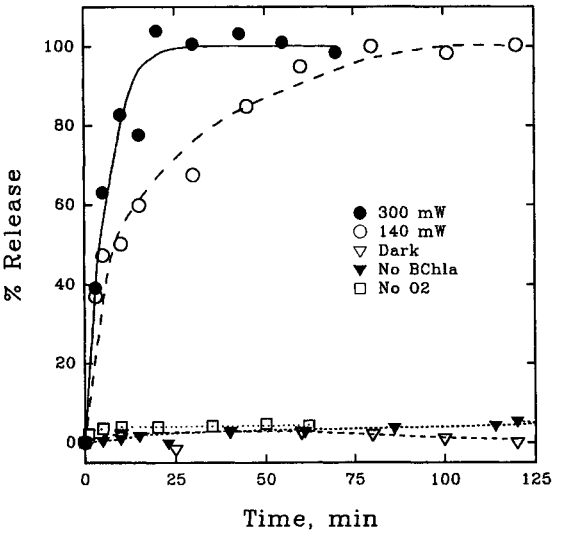

Fig. 6. BChla-sensitized release of calcein from PlsPamCho liposomes (15 μM BChla, 13.9 mM PlsPamCho in 100 mM NaCl/20 mM Tris) irradiated at 39°C (λ = 800 nm). ●, incident light power 300 mW; ○, incident light power 140 mW; ▽, dark control; ▼, 300 mW incident light power, but no BChla; □, 300 mW incident light power and BChla present, but oxygen was removed by 20 min argon purge prior to illumination.

3.1.3. BChla sensitization

Very lipophilic chromophores such as ZnPc and $SnCl_2Pc(OBu)_8$ may not be efficient sensitizers of plasmenylcholine photooxidation due to their localization near the center of the bilayer [38]. Since the plasmenyl 1′-alkenyl linkage is adjacent to the phosphoglycerol backbone, reactive oxygen species such as $^1O_2$ generated near the interlamellar region can physically deactivate within the hydrocarbon region or react to give (non-surfactant) allylic hydroperoxide products before encountering the electron-rich vinyl ether bond near the hydrophilic interfacial region. The effect of sensitizer orientation within the membrane on photostimulated release kinetics from PlsPamCho liposomes, therefore, was probed using BChla, an interfacially-bound sensitizer capable of generating singlet oxygen [39] upon near-IR excitation. Calcein release kinetics for BChla/PlsPamCho liposomes, irradiated under conditions of temperature and laser power identical to those used for $SnPc(OBu)_8Cl_2$/PlsPamCho liposomes are shown in Fig. 6. The observed release rates were power dependent; when 300 mW incident light intensity was used, photorelease was essentially complete within 20 min, whereas photorelease was approximately 60% at the same time interval using 140 mW illumination. Non-irradiated

and irradiated controls (O_2-free and BChla-free) resulted in low background leakage rates (Fig. 6). Lipid photooxidation products and lysolipids were detected by TLC and HPLC [33]. It should also be noted that the photolyzed lipid dispersions remained homogeneous throughout the course of illumination. Aggregation and precipitation of the lipid, however, typically occurred in the dark within 4–24 h after illumination and calcein release were complete.

The crucial role of plasmenylcholine lipids in effecting phototriggered contents release was verified by photolyzing BChla/egg lecithin liposomes containing calcein under the same experimental conditions as shown in Fig. 6. Egg lecithin was chosen since it contains a high proportion of unsaturated fatty acid residues (predominantly oleoyl at the *sn*-2 position), but no vinyl ether linkages. Although photostimulated calcein release did occur from BChla/egg lecithin liposomes ($< 6\%$ after > 100 min illumination; Fig. 7), the observed rate was approximately two orders of magnitude slower than the BChla/PlsPamCho release rate (Fig. 6). These results suggest that reactive oxygen species attack of the plasmenylcholine vinyl ether bond is much more effective at initiating liposome leakage than other lipid oxidation pathways since vinyl ether oxidation generates single chain surfactants. The single chain photolysis products that are formed eventually destabilize the liposome membrane via lamellar defects, such as interlipidic particles, which can mediate liposome permeability and membrane fusion processes.

Light-induced morphological changes in BChla/PlsPamCho liposomes were indicated by ^{31}P-NMR experiments in the presence and absence of Mn^{2+} as line broadening agent (Fig. 8). Non-photolyzed samples show isotropic ^{31}P signals (Fig. 8a, $-h\nu, -Mn^{2+}$) characteristic of phosphorus sites involved in particle tumbling or rapid diffusional exchange that are typically found in unilamellar liposomes. Addition of manganese(II) chloride linebroadened the phosphorus sites in the outer liposome monolayer; the residual signal is attributed to inner monolayer phosphorus. The relative signal intensities after Mn^{2+} addition suggests a 56:44 ratio of outer:inner phosphorus sites, consistent with a 870 ± 90 Å diameter liposome that is not permeable to Mn^{2+} ion prior to photolysis (Fig. 8b, $-h\nu, +Mn^{2+}$). This estimate is in good agreement with the 865-Å size determined by quasielastic light scattering. BChla/PlsPamCho liposomes photolyzed for 75 min (39°C, 300 mW at 800 nm) have axially symmetric powder pattern lineshapes with a superimposed isotropic component 28 h after illumination (Fig. 8c, $+h\nu, -Mn^{2+}$), indicative of a multilamellar phosphorus environment that coexists with a rapidly tumbling component that can be attributed to either partially photolyzed liposomes or interlipidic particles (or both). The increased permeability of photolyzed PlsPamCho membranes is clearly evident upon addition of Mn^{2+} (Fig. 8d, $+h\nu$, $+Mn^{2+}$) since all phosphorus sites are completely line broadened in the manganese-containing, photolyzed BChla/PlsPamCho sample.

Cryo-TEM images of an extruded BChla/PlsPamCho sample taken at various time intervals during illumination

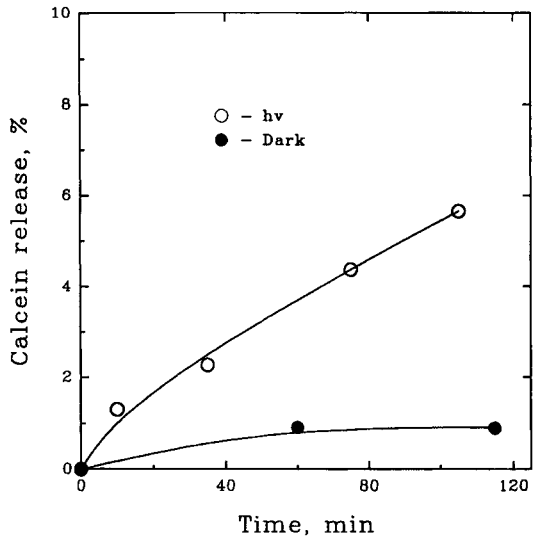

Fig. 7. Release of calcein from BChla/egg lecithin liposomes irradiated at 39°C ($\lambda = 800$ nm, incident light power 300 mW). ○, light-induced release; ●, dark control. All conditions are as described in Fig. 6, except egg lecithin was used to prepare liposomes instead of PlsPamCho at the same [lipid] expressed as mg/ml. (Note differences in *y*-axes in Fig. 6 and 7.)

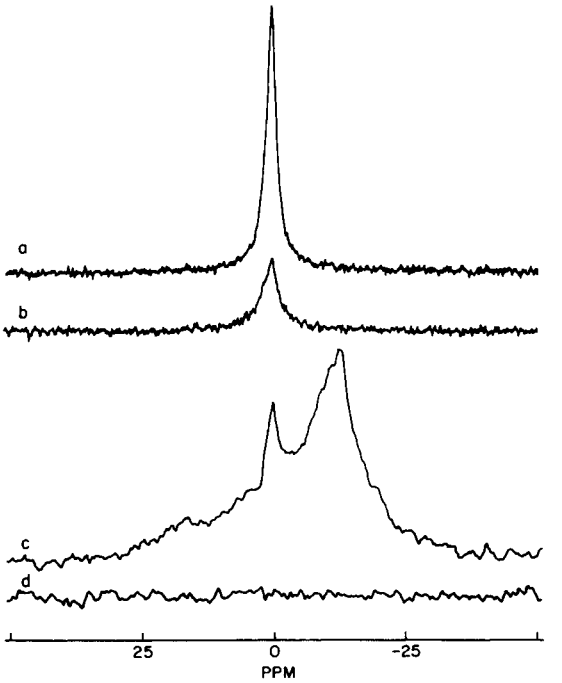

Fig. 8. ^{31}P-NMR spectra of nonphotolyzed (a,b) and photolyzed (c,d) samples of BChla/PlsPamCho liposomes in the absence (a,c) and presence (b,d) of 5 mM $MnCl_2$. Conditions: 15 μM BChla, 16.7 mM PlsPamCho in 100 mM NaCl/20 mM Tris; 75 min illumination: ($\lambda = 800$ nm, incident light power 300 mW; 39°C).

(Fig. 9A–C) depict intermediate stages in the liposomal membrane fusion process. Prior to irradiation, unilamellar liposomes are the predominant species in solution at 38°C (Fig. 9A). Upon irradiation at 150 mW, aggregation of intact liposomes occurs during the first 5 min of photolysis (Fig. 9B, micrograph recorded after a 10 min dark incubation at 22°C). A great reduction in the liposome density was observed, with concomitant appearance of enlarged lamellar vesicles (some exceeding 1 μm in diameter) after 5 min irradiation and 65 min dark incubation at 38°C (Fig. 9C). Aggregated liposomes of heterogeneous diameters and multilamellar rod-like objects (apparently comprised of stacked, 'deflated' liposomes) were also observed. Non-photolyzed samples, on the other hand, appear unchanged after 24 h incubation in the dark at either temperature (22°C or 38°C). Furthermore, the ^{31}P linewidth at half peak height decreases during the course of the photolysis (2.3 ppm at $t = 0$ and 1.5 ppm at 150 min irradiation/440 min dark at 39°C), indicating the presence of phosphorus sites undergoing rapid exchange, which evolve into the aggregate isotropic and axially symmetric powder patterns observed at 28 h (Fig. 8). This evidence, together with cryo-TEM, freeze-fracture TEM, and Mn^{2+} linebroadening results, suggests that a significant fraction of the photooxidized sample exists as micelles, interlipidic particles, or highly fluidized lamellar structures. These intermediate states, however, we believe are transient species that are undergoing a complex transition from intact liposomes to photolyzed multilamellae and interlipidic particles in a kinetic process that is slower than the timescale for contents release.

3.1.4. Comparison of photorelease via ZnPc, $SnCl_2Pc(OBu)_8$ and BChla sensitization

Since the experimental conditions for the different sensitizer/PlsPamCho formulations varied significantly, direct quantitative comparisons between their ability to trigger calcein release are not possible. A number of experimental factors were responsible for these variations. First, differences in the absorption spectra of the dyes (see Fig. 2) required the use of a filtered halogen/tungsten source rather than diode laser excitation for ZnPc samples. In addition, the poor solubility of $SnCl_2Pc(OBu)_8$ in the lipid membrane limited the amount of sensitizer that could be employed in the experiments shown in Fig. 5; the maximum possible concentration of $SnCl_2Pc(OBu)_8$ that could be incorporated within PlsPamCho liposomes, based on simple partitioning, was 8-fold lower than for ZnPc. Experiments with BChla (Fig. 6), however used considerably higher concentrations of sensitizer (BChla can be incorporated into liposomes at very high concentrations; 1:100 BChla/lipid molar ratios are easily attainable). Since BChla is far more prone to photodegradation than are phthalocyanines, higher initial concentrations are required for effective photosensitization. In fact, when illuminated at low concentrations (less than ca. 2 μM BChla), rapid photodegradation occurred without significantly enhancing liposome permeability. These practical considerations permit only the following qualitative comparisons.

(1) The BChla-based liposomes are by far the most efficient photoreleasing system. Since the quantum yields for singlet oxygen formation are not dramatically different for the three sensitizers (0.3, 0.56, and 0.4, for BChla [40], $SnCl_2Pc(OBu)_8$ [31], and ZnPc [41] respectively), a synergism of the following factors can account for this: (a) localization of BChla near the vinyl ether linkage, resulting in a more effective coupling of the singlet oxygen formation and plasmenylcholine oxidation processes at the membrane/water interface; (b) high BChla concentrations in the membrane compared with ZnPc and $SnCl_2(OBu)_8$; (c) good molar absorptivity of BChla at 800 nm; and (d) high intensity source emitting at 800 nm to efficiently drive the photochemistry.

(2) $SnCl_2Pc(OBu)_8$ is a more effective sensitizer than ZnPc. Since $SnCl_2Pc(OBu)_8$ also has high molar absorptivity at 800 nm, it is more effective at triggering plasmenylcholine liposomes than ZnPc due to a more favorable absorption cross section of $SnCl_2Pc(OBu)_8$ with the Al/Ga/As laser source, even when the ZnPc concentration is nearly an order of magnitude higher.

(3) The photostability of phthalocyanines, along with their favorable spectral characteristics and high quantum yields for singlet oxygen sensitization, make them attractive photodynamic therapy sensitizers. A potential disadvantage of their high photostability, however, may be Photofrin-like extended tissue retention times and latent photosensitivity due to retained, intact chromophore. In this regard, the poor photostability of BChla may prove advantageous in the context of practical liposomal-based antitumor phototherapy.

3.2. Photorelease pathway

A conceptual model for liposomal fusion and contents release is proposed in Fig. 10. This model incorporates lipid photodegradation, liposomal aggregation, contents leakage, and membrane fusion steps to account for all our experimental observations. These steps are:

(1) Lipid photodegradation to single chain surfactants (Fig. 10, $h\nu$ step). Efficient photorelease involves the production of single chain surfactant species such as lysolipid and fatty aldehyde.

(2) The formation of membrane defects (Fig. 10, post-$h\nu$ step). Lateral diffusion of the degradation products within the plasmenylcholine liposome and interliposome exchange processes, leading to the accumulation of lysolipid and fatty aldehyde-rich domains that can support interlipidic particle formation within the photolyzed bilayer.

(3) Contents leakage (Fig. 10, pre- and post-fusion steps). Contents leakage occurs rapidly from photolyzed liposomes, presumably through single chain surfactant-stabilized membrane defects, regardless of the starting

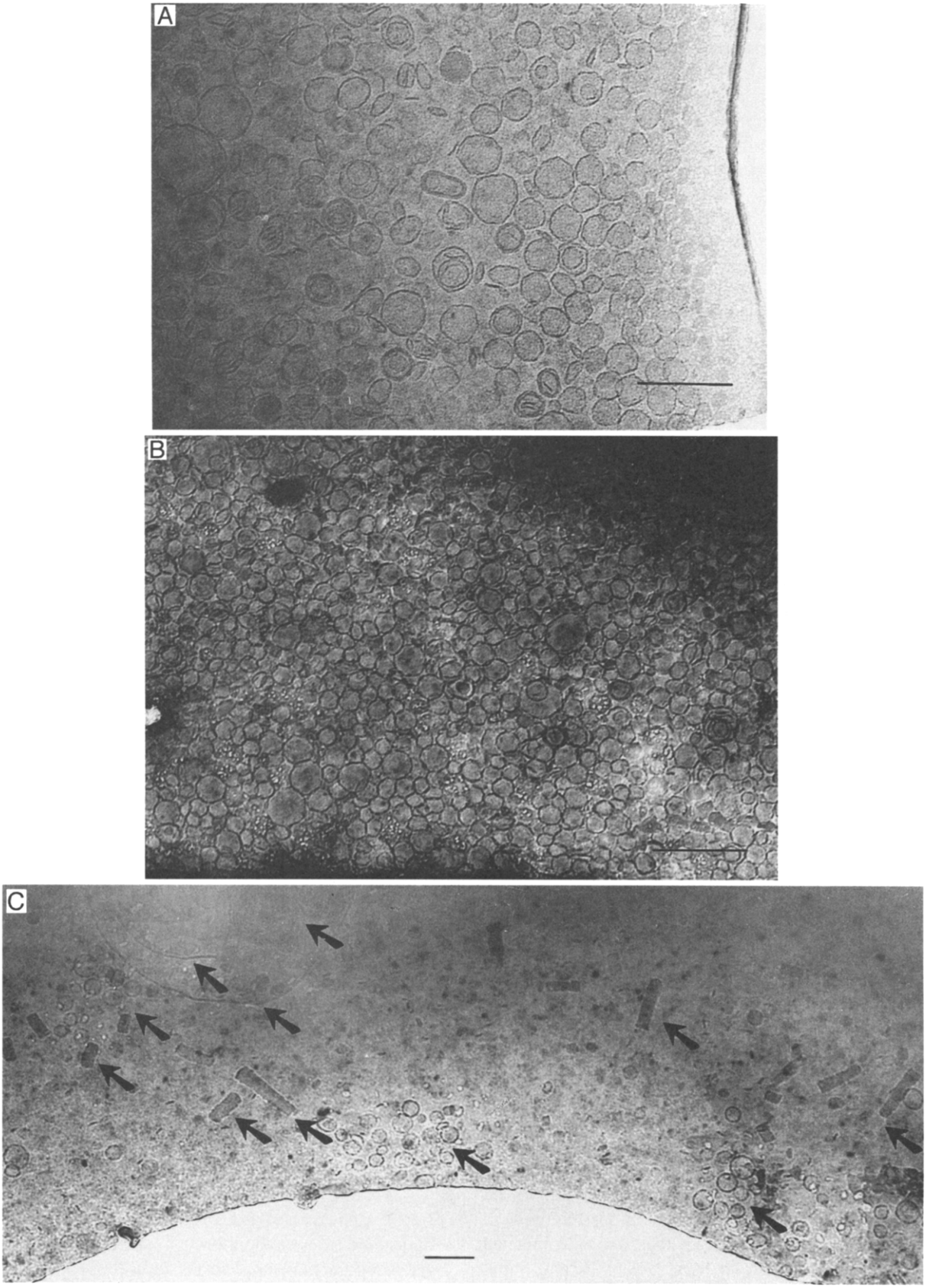
A
B
C

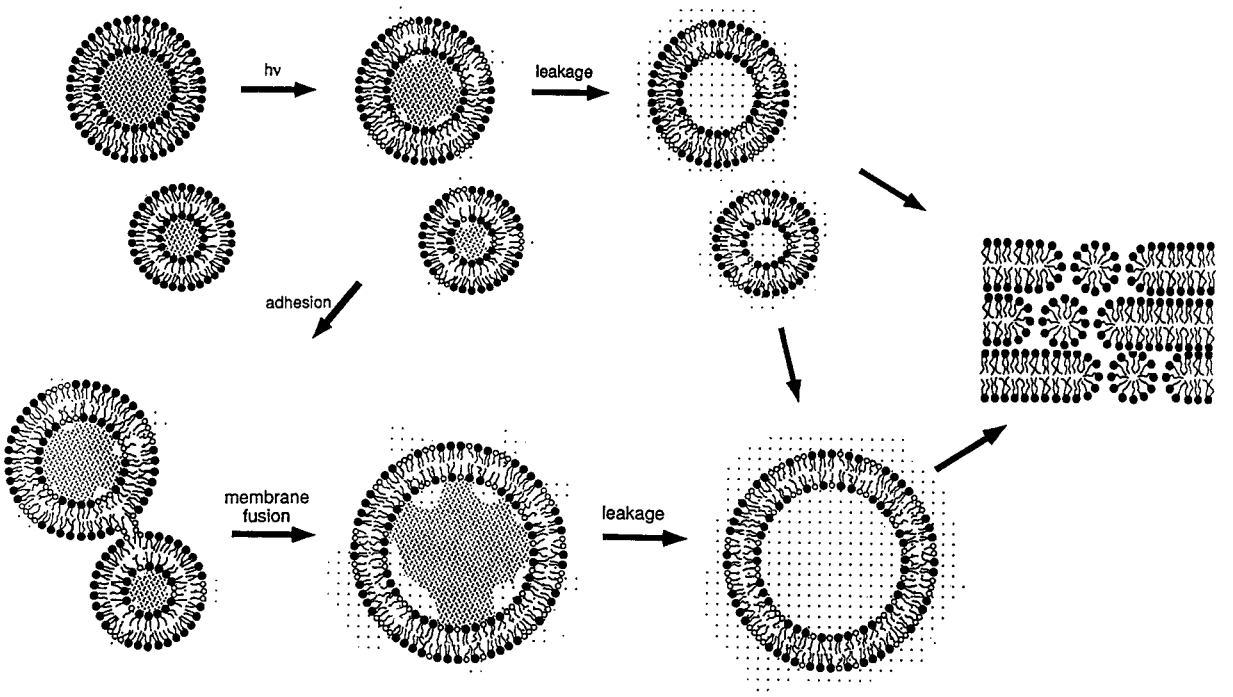

Fig. 10. Conceptual model for liposome aggregation, interlipidic particle formation and membrane fusion. Amphiphile notation: Solid circles with two alkyl tails = intact plasmalogens; Open circles with one alkyl tail = single chain plasmenylcholine photoproduct. Densely shaded areas = intraliposomal contents at high concentration; lightly shaded areas = released liposomal contents at lower concentration.

liposome concentration. Although contents leakage has been observed in all plasmenylcholine liposome systems investigated to date [26,27], the rates of release vary according to sensitizer, contents, concentrations, and other experimental conditions [33].

(4) Liposomal aggregation and membrane fusion (Fig. 10, adhesion and fusion steps). Aggregation and fusion of photolyzed liposomes occurs as a parallel process to contents leakage at moderate-to-high initial lipid concentrations due to increased rates of interliposomal encounter. These phenomena are presumably facilitated by bilayer contact at the lysolipid/fatty aldehyde-rich domains (pores) and interlipidic particle inclusion sites [42]. Our data on concentrated plasmenylcholine liposome solutions (> 5 mM) suggest that aggregation occurs on a similar kinetic timescale as leakage (c.f. calcein release kinetics in Fig. 6 and cryo-TEM images of the liposome solution during illumination in Fig. 9A–C).

(5) Macroscopic aggregation and precipitation of multilamellar lipid (Fig. 10, final step). The endpoint of the photolyzed lipid dispersion is the same regardless of whether adsorption and fusion of the membrane vesicles occurs during or after contents leakage. In both cases, the final lipid state is multilamellar (Figs. 4 and 8c, and Fig. 9C).

Unlike many other systems where membrane fusion is attended by very little contents leakage, our system involves leakage and fusion as simultaneous, independent processes. It is likely that the relative rates of leakage and fusion may vary depending on experimental conditions such as sensitizer localization, sensitizer concentration, temperature, total lipid concentration, light fluency, and the hydrophilic/hydrophobic balance of the encapsulated contents. This is underscored by the observation that contents leakage was only observed when the BChla content in BChla/plasmenylcholine liposomes exceeded 1:4000; photodegradation of the sensitizer during the course of the illumination at lower BChla compositions may prevent the formation of sufficient concentrations of lysolipid and fatty aldehyde to allow for interlipidic particle formation and appreciable contents leakage rates.

4. Conclusions

These results indicate that liposomal leakage, induced by photooxidative cleavage of the plasmenylcholine vinyl ether linkage, is accompanied by liposome aggregation and membrane fusion. Stabilization of membrane defects (such as interlipidic particles or pores at contact points between adjoining liposomes) by single chain surfactants accumulated during plasmenylcholine photooxidation, and acceler-

Fig. 9. CryoTEM of photolyzed (150 mW at 38°C) BChla/PlsPamCho liposomes (0.1 μ Nucleopore filters 25 μM BChla, 19.5 mM PlsPamCho in 100 mM NaCl/20 mM Tris). (A) Before irradiation. (B) 5 min irradiation, 10 min incubation at 22°C. (C) 5 min irradiation, 65 min incubation at 38°C. Scale bars = 2000 Å.

ation of transmembrane flux of encapsulated materials through them, is inferred on the basis of freeze-fracture/freeze-etch TEM microscopy, TLC data (wherein PlsPamCho is degraded to more polar constituents), and ^{31}P-NMR experiments. Since the observed contents release rate depends on a host of factors, in vivo application of this liposomal triggering technique will require optimization for the encapsulated substance of interest and the desired rate of release. In particular, when applying the photooxidative triggering approach to the release of drugs or other biologically active materials, special attention will need to be focused on the relative rates of contents leakage, membrane fusion, and encapsulated contents oxidation during the course of irradiation.

Acknowledgements

This work was supported by grants from the Whitaker Foundation and the Purdue Research Foundation (D.H.T.) and by a grant from the National Research Council as part of the Cooperation in Applied Science and Technology Visiting Scientist Program (D.H.T./O.V.G.). The helpful discussions and kind hospitality provided by Pieter Cullis of the University of British Columbia during a sabbatical leave (D.H.T.) are gratefully acknowledged. The authors also thank Barbara L.-S. Mui and Kim Wong for assistance with preliminary electron microscopy experiments and Donald Eagle, Steven Funk, and Yuanjin Rui for sensitizer and plasmenylcholine syntheses.

References

[1] Harrigan, P.R., Wong, K.F., Redelmeier, T.E., Wheeler, J.J. and Cullis, P.R. (1993) Biochim. Biophys. Acta 1149, 329–338.
[2] Blume, G. and Cevc, G. (1990) Biochim. Biophys. Acta 1029, 91–97.
[3] Allen, T.M., Hansen, C., Martin, F., Redemann, C. and Yau-Young, A. (1991) Biochim. Biophys. Acta 1066, 29–36.
[4] Papahadjopoulos, D., Allen, T., Gabizon, A., Mayhew, E., Matthay, K., Huang, S.K., Lee, K.-D., Woodle, M.C., Lasic, D.D., Redemann, C. and Martin, F.J. (1991) Proc. Natl. Acad. Sci. USA 88, 11460–11464.
[5] Gabizon, A. and Papahadjopoulos, D. (1992) Biochim. Biophys. Acta 1103, 94–100.
[6] Milhaud, P.G., Machy, P., Lebleu, B. and Leserman, L. (1989) Biochim. Biophys. Acta 987, 15–20.
[7] Liu, D., Mori, A. and Huang, L. (1992) Biochim. Biophys. Acta 1104, 95–101.
[8] Mayer, L.D., Tai, L.C.L., Ko, D.S.C., Masin, D., Ginsberg, R.S., Cullis, P.R., and Bally, M.B. (1989) Cancer Res. 49, 5922–5930.
[9] Mayhew, E.G., Lasic, D., Babbar, S. and Martin, F.J. (1992) Int. J. Cancer 51, 302–309.
[10] Allen, T.M. and Chonn, A. (1987) FEBS Lett. 223, 42–46.
[11] Bally, M.C., Nayar, R., Masin, D., Hope, M.J., Cullis, P.R. and Mayer, L.D. (1990) Biochim. Biophys. Acta 1023, 133–139.
[12] Lee, K.-D., Hong, K. and Papahadjopoulos, D. (1992) Biochim. Biophys. Acta 1103, 185–197.
[13] Woodle, M.C. and Lasic, D.D. (1992) Biochim. Biophys. Acta 1113, 171–199.
[14] Vaage, J., Mayhew, E., Lasic, D. and Martin, F. (1992) Int. J. Cancer 51, 942–948.
[15] Litzinger, D.C. and Huang, L. (1992) Biochim. Biophys. Acta 1113, 201–227.
[16] O'Brien, D.F. and Tirrell, D.A. (1993) in Bioorganic Photochemistry, Vol. 2 (Morrison, H., ed.), pp. 111–167, Wiley, New York.
[17] Chu, C.-J. and Szoka, F.C. (1994) J. Liposome Res. 4, 361–395.
[18] Gerasimov, O.V., Rui, Y. and Thompson, D.H. (1996) in Liposomes (Rosoff, M., ed.), Marcel Dekker, New York, in press.
[19] Huang, S.K., Stauffer, P.R., Hong, K., Guo, J.W.H., Phillips, T.L., Huang, A. and Papahadjopoulos, D. (1994) Cancer Res. 54, 2186–2191.
[20] Unezaki, S., Maruyama, K., Takahashi, N., Koyama, M., Yuda, T., Suginaka, A. and Iwatsuru, M. (1994) Pharm. Res. 11, 1180–1185.
[21] Hayata, Y. and Ono, J. (1990) in Medical Laser Endoscopy (Jensen, D.M. and Brunetaud, J.M., eds.), pp. 313–330, Kluwer, Dordrecht.
[22] McCaughan, J.S. (1990) in Photodynamic Therapy of Neoplastic Disease (Kessel, D., ed.), pp. 21–41, CRC Press, Boca Raton.
[23] Wilson, B.C. (1989) in Photosensitizing Compounds: Their Chemistry, Biology and Clinical Use Ciba Foundation Symposium 146, p. 60–77, Wiley, Bath.
[24] Parrish, J.A. and Wilson, B.C. (1991) Photochem. Photobiol. 53, 731–738.
[25] Lenz, P. (1992) Phys. Med. Biol. 37, 311–324.
[26] Anderson, V.C. and Thompson, D.H. (1992) Biochem. Biophys. Acta 1109, 33–42.
[27] Anderson, V.C. and Thompson, D.H. (1992) in Macromolecular Assemblies (Stroeve, P. and Balazs, A., eds.), ACS Symposium Series 493, pp. 154–170, American Chemical Society, Washington.
[28] Morand, O.H., Zoeller, R.A. and Raetz, C.R. (1988) J. Biol. Chem. 263, 11597–11606.
[29] Zoeller, R.A., Morand, O.H. and Raetz, C.R. (1988) J. Biol. Chem. 263, 11590–11596.
[30] Scherrer, L.A. and Gross, R.W. (1989) Mol. Cell. Biochem. 88, 97–105.
[31] Rihter, B.D., Kenney, M.E., Ford, W.E. and Rodgers, M.A.J. (1990) J. Am. Chem. Soc. 112, 8064–8070 and references therein. These sensitizers are now commercially available from Aldrich Chemical Company.
[32] Hope, M.J., Bally, M.B., Webb, G. and Cullis, P.R. (1985) Biochim. Biophys. Acta 812, 55–65.
[33] Gerasimov, O.V., Schwan, A. and Thompson, D.H., unpublished data.
[34] Hope, M.J., Wong, K.F. and Cullis, P.R. (1989) J. Electron Microsc. Tech. 13, 277–287.
[35] Thompson, D.H., Wong, K.F., Humphry-Baker, R., Wheeler, J.J., Kim, J.-M. and Rananavare, S.B. (1992) J. Am. Chem. Soc. 114, 9035–9042.
[36] Verkleij, A.J. (1984) Biochim. Biophys. Acta 779, 43–63.
[37] Arvidson, G., Brentel, I., Khan, A., Lindblom, G. and Fontell, K. (1985) Eur. J. Biochem. 152, 753–759.
[38] Armitage, B. and O'Brien, D.F. (1992) J. Am. Chem. Soc. 114, 7396–7403 and references therein.
[39] The localization of BChla in lipid bilayers should be very similar to that observed for chlorophylls. It has been shown that chlorophylls *a* and *b* are localized in the polar region of the membrane: (a) Oettmeier, W., Norris, J.R. and Katz, J.J. (1976) Biochem. Biophys. Res. Commun. 71, 445–451; (b) Luisetti, J., Mohwald, H., Galla, H.J. (1977) Biochem. Biophys. Res. Commun. 78, 754–760; (c) Funfschilling, J. and Walz, D. (1983) Photochem. Photobiol. 38, 389–393.
[40] Borland, C.F., McGarvey, D.J., Morgan, A.R. and Truscott, T.G. (1988) J. Photochem. Photobiol. B 2, 427–435.
[41] Valduga, G., Nonell, S., Reddi, E., Jori, G. and Braslavsky, S.E. (1988) Photochem. Photobiol. 48, 1–5.
[42] Zimmerberg, J., Vogel, S.S. and Chernomordik, L.V. (1993) Annu. Rev. Biophys. Biomol. Struct. 22, 433–466.